

Study of the effect of the microfluidic effect on reducing the reaction times

Shishanov Mikhail Valentinovich¹, Cook Christopher German^{1}*

¹D.I. Mendeleev University of Chemical Technology of Russia, 125047, Moscow, Miusskaya Square, 9, Russia

Abstract. This study investigated the possibility of generating cavitation effects in microfluidic reactors at sharp pressure drops (from 10 to 1 atm.) without the use of ultrasonic sources. The calculations revealed that with the parameters characteristic of microfluidic systems (channel diameter of 1 mm, flow rate of 100 ml/h), an energy dissipation rate of approximately 3.225 W/cm² was achieved. This value exceeds the known cavitation threshold for aqueous solutions and is within the interval characteristic of cavitation induced by high-frequency sources. A decrease in the diameter of the channel contributes to an increase in specific power, thereby increasing the probability of cavitation. The dependencies of the kinetics of the first-order reaction on the intensity of cavitation were determined. At $\alpha = 0.8$ (cavitation amplification coefficient selected from the literature), the velocity constant increases from 0.010 to 0.0358 s⁻¹, which leads to a significant reduction in the time required to achieve a given degree of transformation.

* Corresponding author: kuk.khristofor@inbox.ru

1 Introduction

Microfluidic technologies demonstrate high efficiency in the implementation of many reaction processes because of their unique properties: a high surface area per unit volume (S/V) and a small diffusion path between reactants. These physical features reduce the resistance to mass transfer and thereby accelerate the initial stages of the reaction [1]. However, as noted by some studies [2], the total acceleration of chemical processes in microchannels often exceeds that which can be explained by diffusion or hydrodynamic advantages alone. It can be assumed that there is an additional mechanism for introducing energy into the reacting system, i.e., viscous energy dissipation in zones of high velocity/pressure gradients.

In microfluidic devices, significant hydrodynamic pressure drops can be observed, up to 10–20 atm. [3], which creates conditions for extreme local dissipation. Its intensity most often significantly exceeds the threshold values (0.3–1 W/cm²) known for the induction of significant nonlinear effects in liquid-phase systems. In this work, a theoretical and experimental attempt is made to prove the effect of this effect on the kinetics of the reaction inside the microfluidic channel without external influence, using the example of liquid-phase production of isophorone.

2 Data and methods

2.1 Initial parameters of the system

A typical microfluidic reactor with the following characteristics was chosen as the object of research and calculations (Table 1):

Table 1. Main features of the microfluidic reactor

Parameter	Designation	Meaning
Inlet pressure	P_1	1.013×10^6 Pa
Outlet pressure	P_2	1.013×10^5 Pa
Pressure drop	ΔP	9.119×10^5 Pa
Volumetric flow rate	Q	2.778×10^{-8} m ³ /s
Channel diameter	d	1×10^{-3} m
Channel length	l	2 m
Reactor volume	V	1.571×10^{-6} m ³
Fluid transit time	τ	56.549 s

On the basis of these conditions, the dissipation energy introduced into the reaction mass was calculated, assuming its complete absorption by the reacting substances.

2.2 Calculation of the dissipation energy

The energy transferred to the fluid (E) was determined as follows (1):

$$E = \Delta P \times V = 1.432 \text{ [J]} \quad (1)$$

The calculation of the dissipation rate (W) is shown below (equation 2):

$$W = E/\tau = 0.025 \text{ [W]} \quad (2)$$

Channel cross-sectional area (S):

$$S = \pi \times d^2/4 = 0.008 \text{ [cm}^2\text{]} \quad (3)$$

The intensity of dissipation (I) is calculated [4] according to equation (4):

$$I = W/S = 3.225 \text{ [W/cm}^2\text{]} \quad (4)$$

Table 2 compares the calculated intensity with the threshold values.

Table 2. Comparison of Design Intensity with Threshold Values

Threshold value	Interval (W/cm ²)
Minimal for significant nonlinear effects	0.3–1.0
To accelerate the chemical reaction	1.0–10.0
Calculated value	3.225

2.3 Experimental procedure in a microcapillary

For studying the process of isophorone production, synthesis was carried out at a laboratory facility, the reactor diagram is provided in Figure 1. 3 ml of 10% NaOH solution was dosed into a container filled with 30 g of water. At the end of the dosing process, the resulting mixture was placed in a syringe with a volume of 150 ml. 75 g of acetone and 15 g of diacetone alcohol were placed in another syringe. The reactor was preliminarily washed with technical acetone. Next, the pumps were connected to the microreactor, the reaction temperature was set from 165 to 200). After 50 minutes required for complete warm-up of the reactor, syringe pumps with a specified flow rate (from 0.5 to 2 ml/min) are turned on. Based on the fluid transit time, wait for two full cycles of liquid dosing. After that, they begin to take samples.

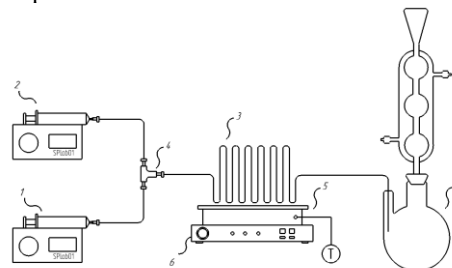


Fig. 1. Method of synthesis of isophorone in microcapillaries using an oil bath: 1,2 – syringe pumps,

3 – 1 mm capillary, 4 – tee, 6 – heating plate equipped with an oil bath 5, 7 – return cooler

The technological process is as follows: the initial components are fed from syringe pumps 1,2 to a stainless steel tee 4, where the primary mixing of the main flows takes place. The mixture is fed into capillary 3, previously bent in the form of a serpentine. The capillary is located in an oil bath 5 equipped with a heating plate 6. Subsequently, the reaction mass enters the flask with a cooler 7.

3 Results

3.1 Diagram of a microfluidic reactor with induction zones

Description: A fluid flow passes through a channel with a diameter of 1 mm. Owing to a sharp pressure drop in individual zones, conditions arise that contribute to a high local intensity of dissipation of the kinetic energy of the flow. The summary diagram (Figure 2) includes three interrelated visuals that reflect the parameters of the microfluidic reactor:

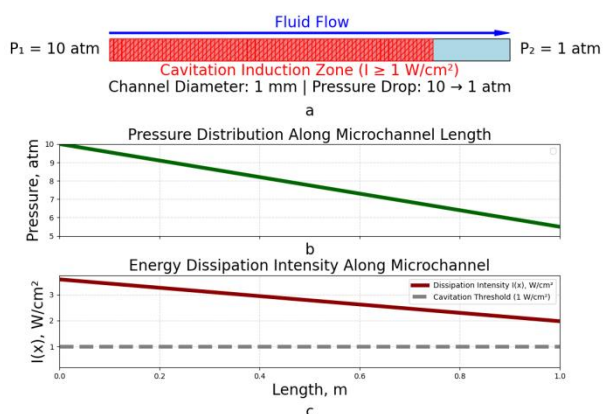


Fig. 2. Summary diagram of calculations: a — diagram of the microchannel with the designation of induction zones at $I \geq 1 \text{ W/cm}^2$; b is the pressure profile $P(x)$; c is the distribution of the intensity of energy dissipation $I(x)$

Figure 2a shows a schematic illustration of a microchannel with the identification of regions of potential zones of significant nonlinear effects that occur when the intensity of energy dissipation is high ($I(x) \geq 1 \text{ W/cm}^2$).

Figure 2b shows the linear pressure profile along the length of the channel ($P(x)$), with a drop from the inlet to the outlet section (10 to 1 atm).

Figure 2c shows a graph of the intensity of energy dissipation ($I(x)$), which is calculated via formula (5):

$$I(x) = \Delta P(x) \times Q/S \quad (5)$$

where $I(x)$ – local intensity of energy dissipation, W/cm^2 ; $\Delta P(x)$ – pressure drop in section (x), Pa.

The diagram shows a good comparison of areas with intensities above the threshold value and the actual induction zones in the microchannel located closer to the output. This confirms the applicability of the computational model for identifying regions of intense

microscale perturbations (IMP) by analysing the pressure and energy distributions along the device.

3.2 Influence of geometry on the intensity of IMP induction

PA comparison of the dissipation rates with changes in channel size and pressure drop was carried out (Figure 3). A decrease in diameter to 0.5 mm leads to an exponential increase in I , confirming the relevance of reducing the channel scale.

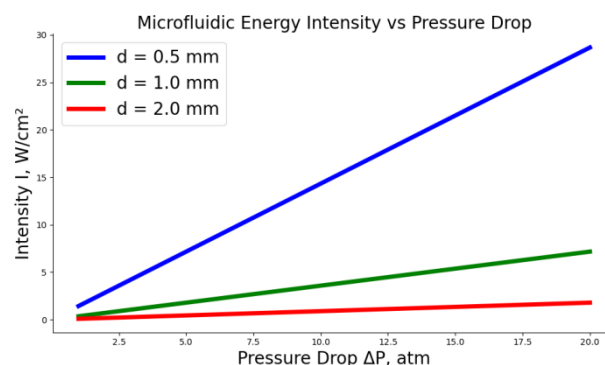


Fig. 3. Dependence of (I) on (ΔP) for different diameters. With a decrease in the diameter of the channel, the intensity increases sharply

3.3 Influence of microfluidic disturbances on the kinetics of the second-order reaction

To do this, let us take the main step of producing isophorone from mesityl oxide from the general reaction scheme (Figure 4):

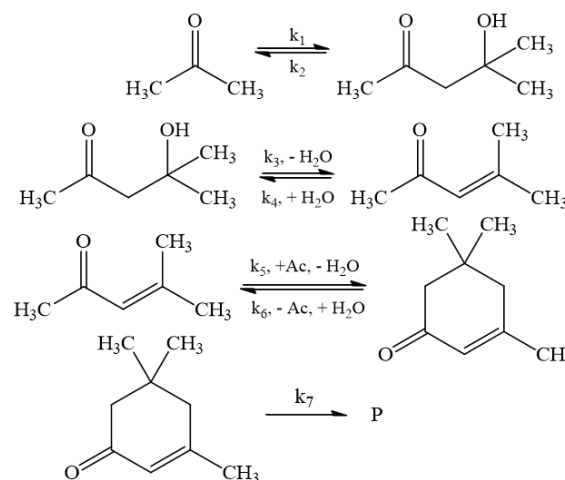


Fig. 4. Mechanism of isophorone production

To quantitatively describe the influence of this dissipation on the reaction rate, we introduced an empirical activation coefficient, α modifying the rate constant as follows:

$$k_{eff} = k \times (1 + \alpha \times I(x)) \quad (6)$$

Where k is the initial reaction constant, α is the dissipation amplification coefficient, and I is the intensity of energy dissipation at a given point in the channel.

In our prior work, we developed and verified a robust kinetic model for the step-wise synthesis of isophorone (via diacetone alcohol and mesityl oxide) in an autoclave, establishing a reliable baseline for the reaction rates under conventional conditions [5].

This provided us with a unique foundation. To assess the effect of hydrodynamic induction on kinetics, systems of differential equations were numerically solved (Figure 5) in two versions: without induction and considering the intensification of the reaction stages.

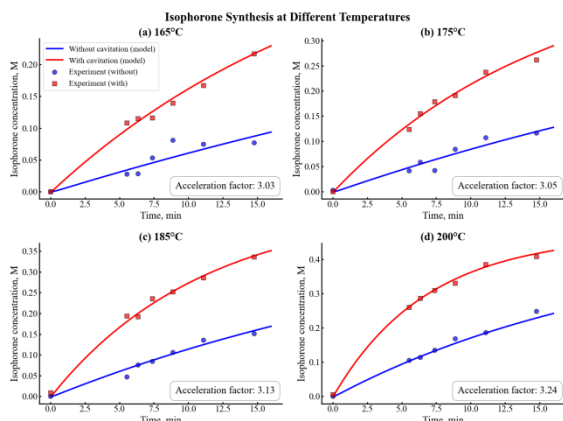


Fig. 5. Comparison of the kinetics of isophorone production without induction and with induction for different temperatures

Moreover, work was carried out to reduce the hydraulic diameter of the capillary by 2 times to determine the effects of geometric parameters on hydrodynamic induction (Figure 6).

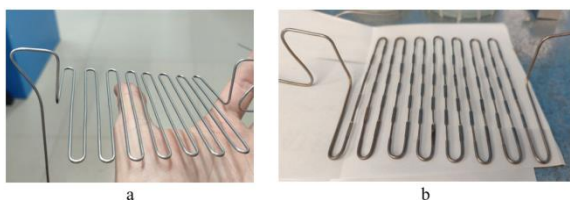


Fig. 6. Modification of the flow part of the capillary: a - standard flow part, b - modified

To systematically investigate the influence of geometric configuration on hydrodynamic induction, the capillary was subjected to a sequential flattening process. This modification was achieved by progressively compressing the original circular capillary (hydraulic diameter $D_h = 1.0$ mm) in two orthogonal planes. Initially, the capillary was flattened along the vertical axis ("top-down" compression) at regular 10 mm intervals along its length. Subsequently, the same procedure was applied along the horizontal axis ("sideways" compression) at identical intervals, resulting in a controlled, anisotropic deformation.

The final geometry approximates a rectangular cross-section with rounded corners. To achieve the target hydraulic diameter of $D_h = 0.5$ mm (a two-fold reduction from the original), the cross-sectional dimensions were designed with a height of approximately 0.4 mm and a width of 0.67 mm. This specific geometry (height: 0.4 mm, width: 0.67 mm) yields the desired $D_h \approx 0.5$ mm, corresponding to a

cross-sectional area reduction of approximately 75% compared to the original circular capillary. The stepwise compression at 10 mm intervals ensured uniform deformation along the capillary length while preventing buckling or flow blockage, thereby creating a well-defined, repeatable microfluidic structure for comparative hydrodynamic studies. Figure 7 shows a comparative diagram of the studies carried out in both types of capillaries.

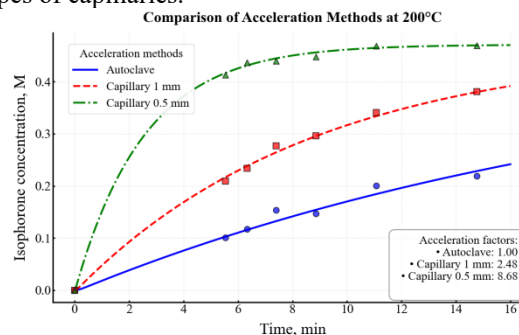


Fig. 7. Comparative diagram: synthesis results in a batch reactor, standard capillary and modified capillary

4 Discussion

The results obtained confirm the key hypothesis of the study: in the conditions of a microfluidic device, it is possible to hydrodynamically initiate effects in liquid-phase systems exclusively owing to a sharp pressure gradient, without the need to use ultrasound or other external sources of energy influence. The intensity of energy dissipation calculated for typical microchannel parameters (inlet pressure of 10 atm, outlet pressure of 1 atm, diameter of 1 mm, and 100 ml/h) was 3.225 W/cm², which not only exceeds the threshold for nonlinear effects in aqueous solutions (0.3–1 W/cm²) but also falls within the range of intensities characteristic of effective reaction acceleration in ultrasonic chemistry [4-7]. A visual visualization of the pressure distribution and induced zones along the length of the microchannel (Figure 1 and Figure 2) demonstrated that the extremum regions are localized closer to the inlet part of the channel, where high pressure values are observed. This coincides with the calculated intensity profile $I(x)$.

In addition, a decrease in the diameter of the channel significantly increases energy dissipation due to an increase in specific power (W/cm²), which makes miniature channels especially promising for the implementation of hydrodynamically induced processes. The study of the effect of induction on the kinetics of the second-order model reaction confirmed that even at moderate values of the hydrodynamic gain factor ($\alpha = 0.637$), the velocity constant increases more than threefold. The effect of cavitation is comparable to that of a significant heating or pressure increase but is achieved locally and without system-wide energy consumption.

Of particular interest is block 3.3, in which a realistic kinetic scheme describing the stages of synthesis of isophorone, an industrially significant compound, was adapted. The use of this scheme from works [8-12] made it possible to extrapolate

microfluidic approaches to more complex reactions, including the formation of intermediate compounds (diacetone alcohol, mesityl oxide). A comparison of the kinetics of isophorone production under conditions with and without induction (Figure 6) revealed an acceleration of the target reaction steps and an increase in the yield of the product in the microchannel subject to hydrodynamic activation. This opens up opportunities to reduce the dwell time in the reaction zone, reduce the channel length and increase the performance of the device while maintaining a high yield.

Thus, microfluidic conditions are an effective solution to the problem of intensifying low-temperature condensation processes, which were previously implemented only in large systems with significant energy consumption. The presented model and calculations serve as justification for the design of compact, energy-efficient reactors, in which hydrodynamics and channel structure become active tools for controlling chemical transformation. Equations should be centred and should be numbered with the number on the right-hand side.

5. Conclusions

1. The theoretical and numerical analysis confirmed the possibility of generating an induced effect in microfluidic reactors due to a sharp pressure drop between the inlet and outlet (from 10 to 1 atm.) without the use of ultrasound or external excitation.

2. The calculated energy dissipation rate was 3.225 W/cm², which exceeds the minimum required for the occurrence of nonlinear effects in an aqueous medium (0.3–1.0 W/cm²) and corresponds to the range in which hydrodynamic induction has a significant effect on the kinetics of chemical reactions (1–10 W/cm²).

3. A direct dependence of the induction intensity on the diameter of the channel and the pressure drop is shown: when the diameter of the channel decreases to 0.5 mm, the intensity increases sharply, which confirms the effectiveness of miniaturization of microfluidic systems for activating reactions.

4. The application of the model to the isophorone synthesis reaction confirmed the practical significance of the hydrodynamic effect in complex reactions: at a given intensity and α gain, an acceleration of key stages and an increase in the yield of the target product are achieved.

5. Visualization of the pressure distribution and cavitation intensity along the microchannel made it possible to identify induction-active zones, which opens up the possibility for targeted optimization of the microfluidic reactor configuration.

7. On the basis of the data obtained, the use of the calculated induction inductions for a preliminary assessment of the reactivity of microfluidic systems, as well as for the selection of optimal geometric parameters of channels and supply conditions, is proposed.

These findings confirm the promise of using hydrodynamic induction in microfluidic technologies as an energy-efficient means of accelerating chemical processes without the need for external excitation and

serve as the basis for the design of new generations of compact reactors.

References

1. W. Liu, J. Li, Z. Chen, Z. Liang, B. Yang, Unveiling the “sono-physico-chemical” essence: Cavitation and vibration effects in ultrasound–assisted processes. *Chin. J. Catal.* **61**, 37-53 (2024). [https://doi.org/10.1016/S1872-2067\(24\)60028-8](https://doi.org/10.1016/S1872-2067(24)60028-8)
2. C. Wang, O. Tao, J. Wu, H. Jiang, Sonochemistry: Materials science and engineering applications. *Coord. Chem. Rev.* **526**, 216-373 (2025). <https://doi.org/10.1016/j.ccr.2024.216373>
3. H. Zheng, Y. Zheng, J. Zhu, Recent Developments in Hydrodynamic Cavitation Reactors: Cavitation Mechanism, Reactor Design, and Applications. *Engineering.* **19**, 180-198 (2022). <https://doi.org/10.1016/j.eng.2022.04.027>
4. L. Liang, Z. Lou, C. Wan, Theoretical estimation of sonochemical characteristics in a single cavitation bubble under various static pressure conditions. *AIP Adv.* **14**, 335-353 (2024). <https://doi.org/10.1063/5.0203571>
5. M.V. Shishanov, Kh.G. Kuk, E.L. Gevorkyan, Kinetic modelling of the reaction of isophorone synthesis. *Chem. Chem. Technol.* **63**, 69-74 (2025). <https://doi.org/10.6060/ivkkt.20256806.7172>
6. M.V. Shishanov, H.G. Kuk, B. Tabura, Y. Zhou, Optimization of the typical condensation process on the example of isophorone synthesis in a microchannel. *Bull. Eng. Res.* **7**, 43-52 (2024). <https://doi.org/10.58224/2619-0575-2024-72-43-52>
7. Kh. Kuk, M.V. Shishanov, K.A. Dosov, D.V. Yashunin, I.A. Bolshakov, N.V. Morozov, Technology of obtaining isophorone in a microfluidic reactor. *Theor. Found. Chem. Eng.* **58**, 277-296 (2024). <https://doi.org/10.31857/S0040357124030023>
8. M. Schröder, T. Bätge, E. Bodenschatz, M. Wilczek, Estimating the turbulent kinetic energy dissipation rate from one-dimensional velocity measurements in time, *Atmos. Meas. Tech.* **17**, 627–657. <https://doi.org/10.5194/amt-17-627-2024, 2024>.
9. L. Xu, X. Yan, Y. Zhang, J. Xu, Y. Zheng, A vortex-enhanced mean kinetic energy method for assessing hydraulic losses in the hump region of pump-turbines. *Sustain. Energy Technol. Assess.* **82**, 104495 (2025).
10. B. Wang, T. Zeng, J. Shang, J. Tao, Y. Liu, T. Yang, H. Ren, G. Hu, Bubble dynamics model and its revelation of ultrasonic cavitation behavior in advanced oxidation processes: A review. *J. Water Process Eng.* **63**, 105470 (2024). <https://doi.org/10.1016/j.jwpe.2024.105470>

11. D. Wang, B. Wei, Y. Xia, L. Jin, B. Wang, B. Dong, H. Gao, F. Shi, From chemical fuels to kinetic energy: Self-propelled macroscopic smart devices. *Adv. Colloid Interface Sci.* **348**, 103728 (2026). <https://doi.org/10.1016/j.cis.2025.103728>
12. G. Xia, W. You, S. Manickam, J.Y. Yoon, X. Xuan, X. Sun, Numerical simulation of cavitation-vortex interaction mechanism in an advanced rotational hydrodynamic cavitation reactor. *Ultrason. Sonochem.* **105**, 106849 (2024). <https://doi.org/10.1016/j.ultsonch.2024.106849>